DESIGN AND EVALUATION OF ACTUATION SYSTEMS FOR POSITION VARIABLE SHOCK CONTROL BUMPS

M. Schäfer[1], S. Lübbe[1], A. Goerttler[2], S. C. Künnecke[3], O. Bertram[1]
[1]German Aerospace Center (DLR), Institute of Flight Systems, Lilienthalplatz 7, 38108 Brunswick, Germany
[2]German Aerospace Center (DLR), Institute of Aerodynamics and Flow Technology, Bunsenstraße 10, 37073 Goettingen, Germany
[3]German Aerospace Center (DLR), Institute of Lightweight Systems, Lilienthalplatz 7, 38108 Brunswick, Germany

Abstract

A shock control bump (SCB) on the wing of a transonic airfoil can reduce the drag coefficient. However, a permanently active bump can also have negative effects and thus cannot be active over the entire flight envelope. Therefore, an adaptive SCB is required to take advantage in certain flight phases without having a negative effect on the flight in other phases. A position variable SCB can cover a larger flight range than a position fixed SCB. The system design process for a position variable SCB is strongly driven by interdisciplinary considerations, as both aerodynamic and structural boundary conditions have to be addressed.

This paper describes the conceptual design process of such an SCB system, with the design of the actuating system and the analysis of the available installation space being the main focus of this work. The process starts with a preliminary design of the kinematic points of the actuation system. From the kinematic design and the provided aerodynamic loads, initial performance requirements for the actuator are derived. In the next step, three-dimensional models of different actuator technologies are automatically generated based on the performance requirements. Within the model environment, an installation space analysis can then be carried out in greater detail to further determine the integrability of the system.

To investigate different concepts and apply the process to different wings, many steps of the process are automated or semi-automated. Based on the system design and the inclusion of aspects from aerodynamics and structure, a concept for a position variable SCB system was defined. Finally, the design was evaluated at aircraft level based on a flight mission.

INTRODUCTION

The aviation industry is a significant contributor to climate change [1], which is why sustainability has become a key focus within the industry. Future propulsion concepts for engines are at the centre of current research, with sustainable aviation fuels and green hydrogen having great potential to reduce emissions [2]. Regardless of the propulsion technology used, the fuel consumption of aircraft must be reduced, as these energy sources are not available in abundance. On the contrary, the production of sustainable fuels is associated with high costs [2]. This would increase the costs for the operation of aircraft and therefore also the costs for the passengers. Accordingly, research must continue on concepts that reduce the drag of the aircraft and thus to reduce fuel consumption. This will allow the economic operation of the aircraft.

In this regard, laminar wings can play an important role in next-generation aircraft, as they significantly reduce the drag coefficient [3]. In addition to laminar flow, a shock control bump (SCB) can be used to further reduce the drag of a transonic wing [4]. The SCB reduces the negative effects of a transonic shock, thereby contributing to a lower drag coefficient. However, in addition to the aerodynamic design of such a bump, a crucial aspect is the integrability of the SCB actuation system into the wing. A structured design approach enables an early review of the system's feasibility on the aircraft. Additionally, the early inclusion of feasibility studies on the system side can prevent later rework and, thus, reduce costs.

This paper presents a model-based design of an actuation system for position variable SCB. The position variability of the bump allows a greater range of application over the flight envelope, but causes greater complexity in system and structure design. In the investigated flight conditions, the compression shock on the transonic wing is located on the outer spoilers. Accordingly, the shock control bump actuation system of the SCB affects the spoiler and its actuation system. This leads to additional complexity of the system design process.

The approach for the conceptual design process described in this paper was developed as part of the Federal Aeronautical Research Program (LuFo) in the project Move-IntegR. The process starts with a preliminary design of the kinematic points of the actuation system. The design of the points is performed in dependence of the wing installation space. From the kinematic design and the provided aerodynamic loads, initial performance requirements for the actuator are derived. In the next step, its components are sized and resulting mass and dimension are computed. From this sizing results three-dimensional models of different actuator technologies are automatically generated. These models enable a fast design and evaluation of actuation concepts in an early design stage. Within the model environment, an installation space analysis is carried out in greater detail to further determine the integrability of the system. A reference system architecture for the overall aircraft is defined to analyse the impact of the new SCB system. Finally, the designed SCB system is evaluated for a defined flight mission.

1. SHOCK CONTROL BUMP DESIGN

The SCB is a bump on the upper side of the wing that can positively influence the flow of transonic airfoils. The bump is positioned in the area of the compression shock to reduce its negative effects. The simplified functionality of an SCB is depicted in figure 1 and described below.

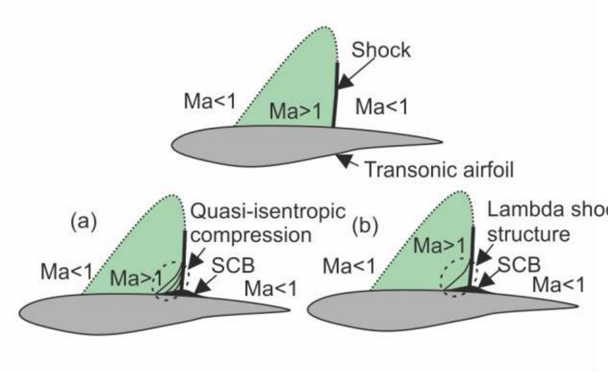

Figure 1: SCB functionality with a quasi-isentropic compression (a) based on [5] and lambda shock structure (b) based on [6]

In the project, the bump is used in the transonic drag rise regime. In this use case, the wave drag which results from the compression shock can be reduced during the flight. Depending on the contour of the SCB, two distinct flow effects can occur (Figure 1: (a) and (b)). The SCB can induce a quasi-isentropic compression marked by numerous weaker shocks (a). Alternatively, a 'lambda shock structure' may emerge (b). Both variations can reduce wave drag on the wing. To exploit this technology optimally, adjustments to the shape, height, and placement of the bump must be made according to flight conditions and application. A detailed description of the aerodynamic functionality can be found in [4].

The configuration of the wing's airfoil significantly influences the variation in shock position. Particularly with turbulent airfoils, shock position variance is sensitive to flight conditions. The design of a fixed position SCB for a laminar wing with an unswept leading edge was investigated in a project previous to Move-IntegR [4]. Move-IntegR itself concentrates on a variable position SCB for a Hybrid Laminar Flow Control (HLFC) wing with a swept leading edge, as it is expected to yield greater benefits for the aircraft. Initial explorations within the project indicate that the shock position at the outer wing area aligns with the spoilers. Consequently, the SCB system must be considered in conjunction with the entire spoiler setup.

There are different concepts for the implementation of the SCB on the spoiler system [7]. In [8], a concept with a pre-bent spoiler is demonstrated which allows a fixed-position bump to be actuated with the spoiler actuator. Thus, by adjusting the spoiler actuator, it is possible to switch between clean configuration and SCB configuration. This solution has the advantage that no additional system components are required, and only the spoiler structure has to be adapted. This concept was further developed in [9]. A second actuator (support actuator) allows creating more than one bump position, which results in a higher range of application. This results in the two-actuator concept consisting of the spoiler actuator, the support actuator, the pre-bent spoiler structure, and the connecting elements (kinematics). As well, control electronics including the necessary sensors must be provided. Both concepts are illustrated in figure 2.

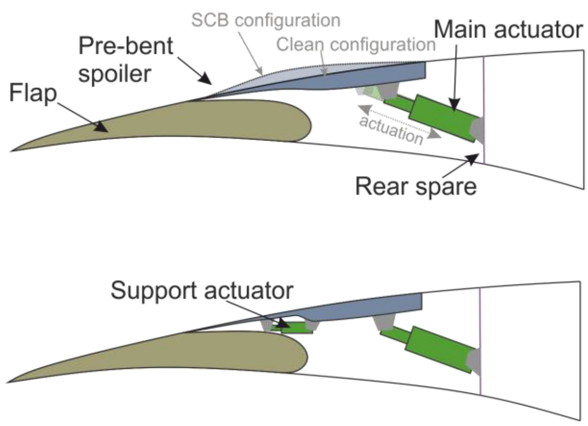

Figure 2: One-actuator concept (top) and two-actuator concept (bottom) for SCB functionality

In the course of the Move-IntegR project, the two-actuator concept was transferred to an HLFC reference wing and further developed. Among other things, the further development includes a detailed consideration of the actuation system and the resulting construction requirements in the wing of the reference aircraft.

2. SYSTEM DESIGN PROCESS

The design process of the Shock Control Bump cannot be completed without considering the aerodynamic and structural properties. Consequently, the design process of an SCB system is highly interdisciplinary and iterative. The main steps of the process are illustrated in figure 3. The starting point is usually the aerodynamic design of the SCB on the aircraft at a given flight point. Even in this stage, structural boundary conditions must be taken into account, as the bump is only permitted to be located on the spoiler.

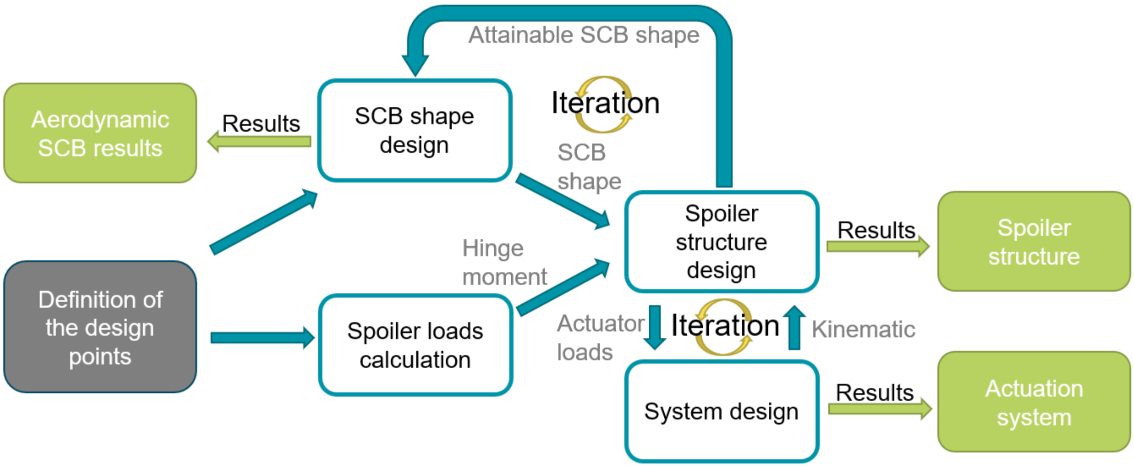

Figure 3: Overall SCB design process

The SCB shape resulting from the aerodynamic optimization process serves as input for the structural design of the pre-bent spoiler. The maximum aerodynamic loads on the spoiler are also necessary to ensure the other spoiler functions, such as the air brake function.

From the system design, initial attachment points of the actuators are provided to estimate the loads on the actuation system. Subsequently, feedback is provided to the aerodynamic design regarding the achievable shape of the SCB. These steps are then repeated until a coherent solution is reached from an aerodynamic, structural and systemic perspective, enabling the determination of a final design for an SCB system.

A detailed description of the aerodynamic and structural results are presented in [10] and [11]. In this work, the primary focus lies in the system design (blue box). This process is also iterative and comprises four main stages, as depicted in Figure 4.

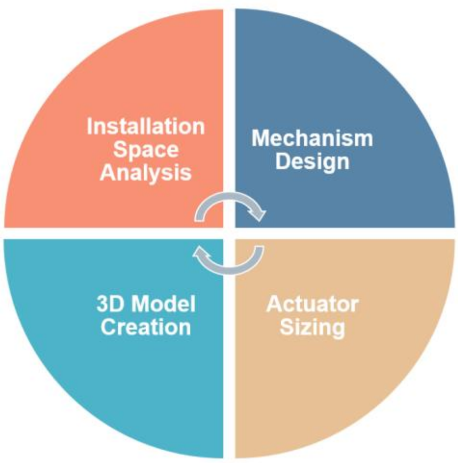

Figure 4: Actuation system design loop

As previously described, the system design process commences with defining the kinematic points based on the available installation space. The resulting loads are subsequently used for the design of the actuation systems. The system designs are then utilized to generate installation space models in a computer-aided design (CAD) tool. In the final step of the process, these space models are integrated into the CAD model of the entire wing in order to verify the design parameters and adjust the positioning of the actuation system. Following the adjustment of the position, the loads and stroke must be determined again. This iterative process continues until convergence is achieved. The individual process steps are elaborated upon in the subsequent sections.

2.1. Mechanism Design

The process commences with defining the attachment points of the actuators to the rear spar and spoiler. The spoiler mechanism, akin to the aileron mechanism, commonly employs a simple hinge mechanism. This involves two attachment points and the pivot point on the spoiler. In the definition of the design space, the installation space and the distance between the points must be considered. The distance between the two attachment points defines the actuator length. Furthermore, it is imperative to ensure non-collision between the structure and the mechanism upon actuator extension.

Derived from these requirements, an algorithm has been devised to determine the mechanism that fits within the available installation space, utilizing a wing section as the foundation. Based on the rear spar and spoiler, two areas are defined with respect to the profile length (see figure 5). These regions can be labelled as the design space (blue and yellow). Within this design spaces, point clouds are defined and all possible connections between the points are investigated. Moreover, boundary conditions are set to limit the minimum and maximum lengths of the actuation system.

Through this exploration, a pair of points is chosen, exhibiting the longest possible lever arm to minimize the load on the actuation system.

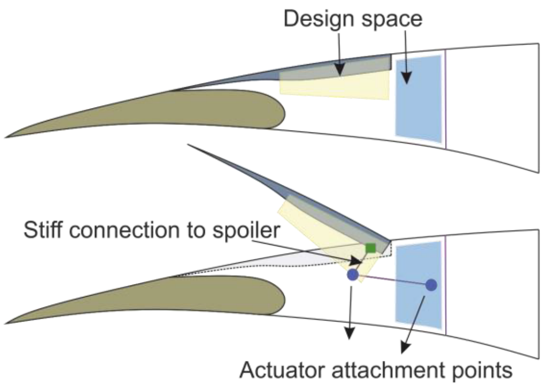

Figure 5: Mechanism design process

Utilizing this method, an initial assessment of the actuator load can be automatically derived across a range of airfoil sections and control surfaces. Furthermore, the applicability of this approach extends to various types of aircraft.

2.2. Actuator Sizing

Initial loads for the actuator design can be determined from both the kinematics and the aero loads. The actuator's required stroke is determined through kinematics, considering the prerequisites for the spoiler's extension angle. Moreover, the control surfaces have a defined deflection speed. Concerning the maximum load, the emergency dive and the holding of the actuators during cruise flight in the clean configuration are usually the dimensioning load cases [12]. For the considered aircraft, the dimensioning scenario is the emergency dive at full actuator stroke.

The maximum deflection speed of the control surface (spoiler) is defined by the flying qualities (e.g. [13]). However, these values are often not available in the early design phase. As a preliminary measure, a full deflection per second can be presumed [12].

Based on this information, the components of the actuators can be initially dimensioned. This dimensioning can be achieved through Commercial Off-The-Shelf (COTS) components and sizing laws, or via elastostatic equations. Throughout the design process, three different actuator technologies are investigated:

- Electro-Hydraulic Servo Actuator (EHSA)
- Electro-Hydrostatic Actuator (EHA)
- Electro-Mechanical Actuator (EMA (geared))

Figure 6 illustrates the structural characteristics of each individual actuator technology.

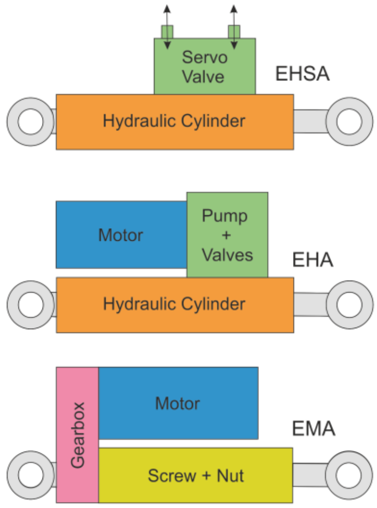

Figure 6: Basic structure of the three investigated actuator technologies: EHSA, EHA, and EMA

EHSA refers to hydraulic cylinders necessitating a hydraulic power supply system. These components mainly consist of a cylinder and a servo valve. They find utility across a wide array of aircraft types. With the ongoing shift toward more electric and all-electric aircraft, electric actuation systems are gaining prominence. Electric actuators find application in the latest aircraft generations such as the Boeing 787 and Airbus A350. They offer benefits such as reduced maintenance costs and overall weight, due to the elimination of hydraulic supply networks required for EHSA operation [14]. However, this advantage only applies when individual hydraulic networks are eliminated due to the number of electric actuators.

EHA is an actuation system consisting of a local hydraulic system, driven directly by a bidirectional pump. The pump is driven by an electric motor. Various combinations are possible, with the combination of a variable speed motor and a fixed displacement pump emerging as the preferred choice for aerospace applications [15]. In contrast, in an EMA the motor's rotational speed is transferred to a linearly moving screw via gearbox, eliminating hydraulic power transformation completely. The rotational movement of the screw is translated into linear motion of the nut or vice versa, with both arrangements being feasible.

The process described here exclusively covers linear actuators, without incorporating specialized designs such as Electric Backup Hydraulic Actuation (EBHA). The dimensioning of EHSA is done by designing the hydraulic cylinder according to [16]. However, the electrical components, pumps, and valves are more complex and are dimensioned using sizing laws and COTS components [17], [18]. A summary of the sized elements for each actuator type and the corresponding references/methods employed is provided in table 1.

Table 1: Actuator sizing methods overview

Type	Elements	Method
EHSA	Cylinder with piston and rod	Elastostatic equations [16]
	Valves	Sizing laws [18]
EHA	Motor	Sizing laws [17]
	Pump	Sizing laws [18]
	Valves	Sizing laws [18]
	Cylinder with piston and rod	Elastostatic equations [16]
EMA	Motor	Sizing laws [17]
	Housing with screw and nut	
	Gearbox	

2.3. 3D Model Creation

After dimensioning the actuators, CAD models are generated based on the calculated data. To realize this process, parameterized installation space models have been designed for each of the three technologies (EHSA, EHA, and EMA). These models are simplified representations of the main components from the sizing process. Each component of an actuator model is defined with variables. Ensuring non-collision of all components regardless of their individual geometric parameters is crucial. A simplified representation supports this procedure. The following three figures illustrate the CAD models of the different technologies.

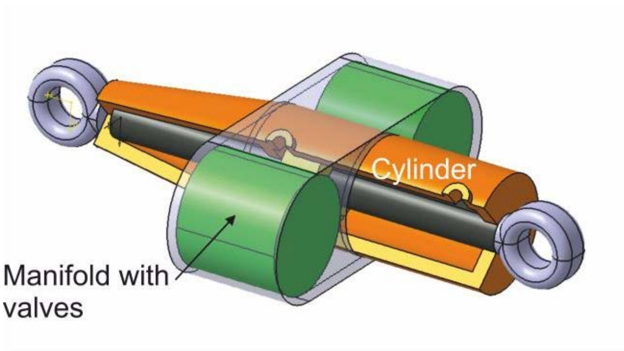

Figure 7: Parametric 3D CAD model of an EHSA

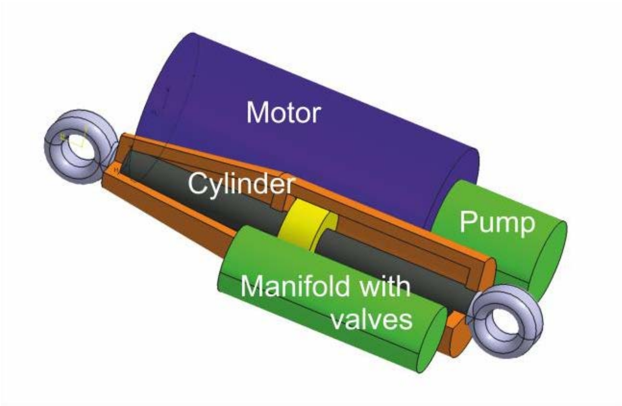

Figure 8: Parametric 3D CAD model of an EHA

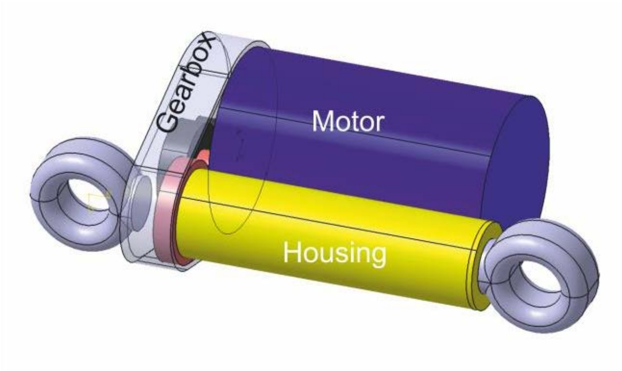

Figure 9: Parametric 3D CAD model of an EMA

The variables of the parametric models are directly linked to the actuator sizing process. As a result, CAD models can be automatically generated from each sizing run, utilizing the specific parameter values.

2.4. Installation Space Analysis

During the final step of the initial iteration, the 3D models are integrated into the CAD model of the wing at the determined positions, as established in the mechanism design section. As the first kinematic design usually only involves a point-dash representation of the actuator, adjustments to the actuator positioning are often necessary. Additionally, the exact minimum length of the actuator might not be known at this stage. These factors can potentially lead to modifications in the positions of kinematic points. As a result, the actuator requirements in terms of force, stroke, and speed might be altered.

Figure 10 shows the actuation system featuring the support actuator within the provided installation space. The actuators implemented in the presented section are EMA. However, an analysis of EHSA and EHA is also possible in the same way.

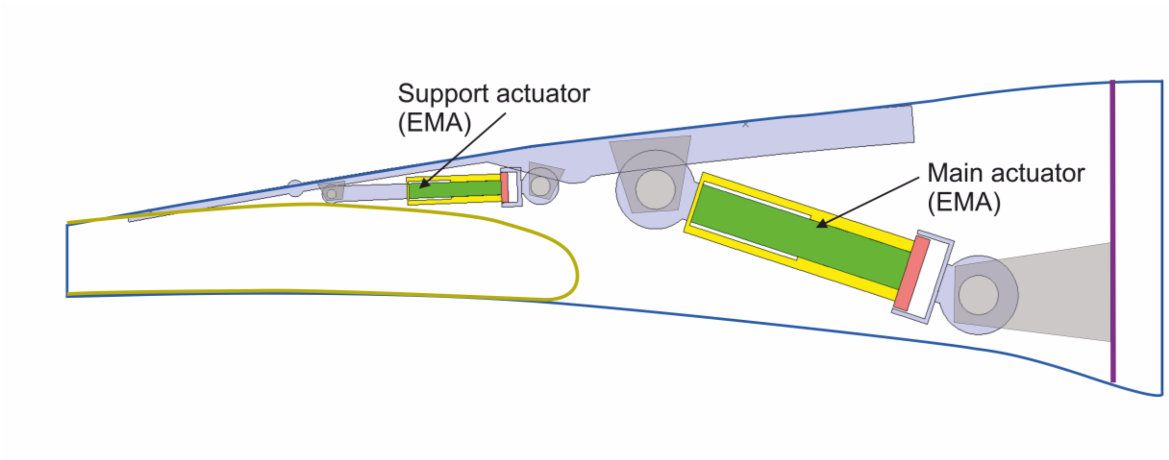

Figure 10: Design space analysis in the CAD model of the wing with parametric actuator models (EMA)

After the manual position adjustments, the process is rerun to align the installation space models with the new requirements. This is done until it is no longer necessary to adjust the kinematic points for the installation space models.

3. SYSTEM DESIGN RESULTS

In order to analyse the results obtained from dimensioning the actuation system, it is essential to establish an aircraft reference architecture. This reference architecture allows for the assessment of how the added system components impact the entire system. In the project a twin aisle aircraft with a purely electrical system architecture was defined. Additionally, the effects on aircraft level are evaluated on the basis of a predefined flight mission. These results are intended to demonstrate the technology's potential and are succinctly discussed in the concluding section of this chapter.

3.1. Reference Aircraft

The aircraft model used for the installation of the SCB system is a scientific model which was created within the framework of the EU CleanSky 2 project [19]. It is a wide body long range aircraft with an HLFC wing. The laminar flow is realized by the HLFC systems developed in the leading edge. The aircraft has two flaps, two ailerons, three slats and six spoilers on each wing. Following the development towards More or All Electric Aircraft the system architecture is defined without hydraulic network and instead with electric actuators. The wing layout with the different control surfaces as well as the corresponding actuator types are shown in figure 11.

Based on the described control surface layout, the architecture of the flight control system's actuation system, and electrical power supply system was designed. Alongside the novel spoiler actuation concept, the assumed redundancy of actuators for the control surfaces was based on current commercial aircraft. For primary flight control, this leads to the assumption of duplex actuation for ailerons and elevators, and triplex actuation of the rudder. Secondary Flight Control was assumed to be realized through parallel active-active actuation of the flaps and slats.

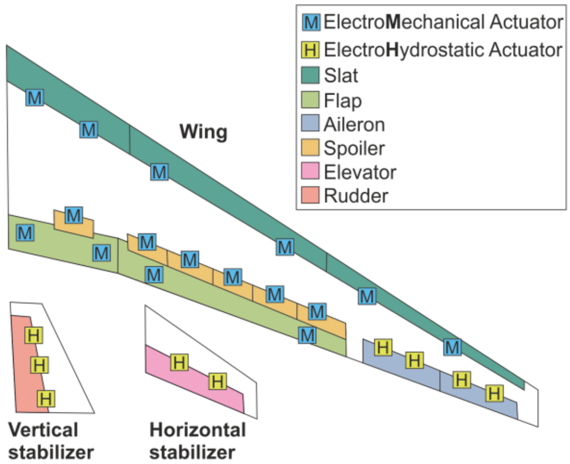

Figure 11: Control surfaces of the HLFC wing with the corresponding actuators

From this starting point different potential architectures for the power supply of the assumed actuation were generated with rising redundancy of supply busses and generators. For all potential architectures minimum achievable probabilities for the loss of roll control, pitch control and yaw control were estimated and used to disqualify unsafe candidates. This approach results in a minimal redundancy supply architecture for the initial design iteration. It contains two segregated power supply busses supplied by at least two generators on each engine and an additional generator supplied by the auxiliary power unit (APU).

The architectures were modeled using the commercial software *Pacelab SysArc*, to simulate different configurations of the power supply over the flight mission and in various failure states. This enables a sizing of the actuators based on their assumed load share and in turn the necessary supply systems, including generators and cables. The electrical power supply consists of five generators, two of which are connected to each engine and one to the APU. The sizing methods used for this purpose correspond to the methods already described in section 3.2.

The definition of the system architecture results in the following mass distribution of the individual system components depicted in figure 12. The collective mass amounts to approximately 3,400 t. Consequently, the primary contributors to this weight include the actuators for the flaps, the generators mass, and the cables mass. The mass of the spoiler actuation is also significant with a share of about 12% (420 kg).

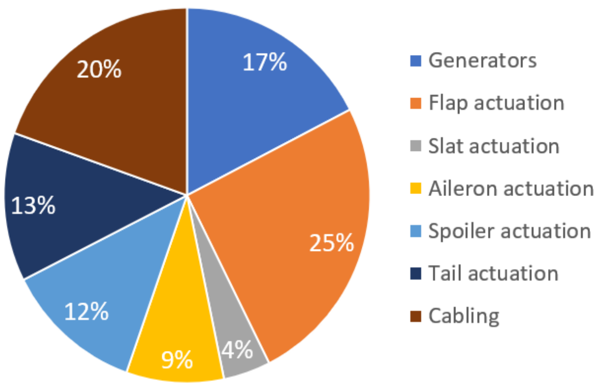

Figure 12: Pie chart of flight control system and electric system mass of reference aircraft

3.2. Analysis Results

The aerodynamic studies have shown that the SCB can be used especially in the outer area of the wing to reduce drag. Therefore, the application of the concept is considered to the four outer spoilers of each wing. In total, the aircraft has eight spoilers that are equipped with additional SCB functionality.

During the installation space analysis, it was determined that the support actuator is too large to fit within the available installation space between the spoiler and the flap. However, this position is necessary in order to generate an aerodynamically favourable SCB. For this reason, instead of a single support actuator, two actuators are finally used for the concept, which share the load. This way, a position is found that fulfils the structural requirements. Accordingly, two support actuators are used per spoiler, totalling in 16 support actuators on the entire reference aircraft.

From the analysis of the basic system architecture and the mass of the actuation systems required for the SCB, it can be concluded that the influence of the additional system is small. With about 3.5 kg per support actuator, this results in a share of about 2% of the considered system mass (figure 13). The mass is low due to the fact that the maximum load is divided between two actuators. Additionally, the speed requirements for the support actuators are low. The SCB holds in a static position over a large flight range. Dynamic movement of the bumps is not necessary according to the design. Accordingly, the power requirement is also low and has no influence on the design of the aircraft generators.

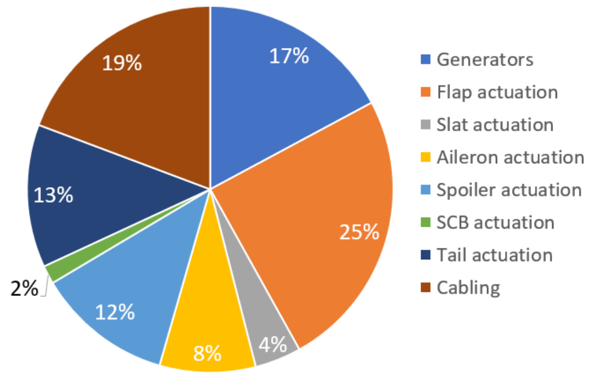

Figure 13: Pie chart of flight control system and electric system mass with SCB system

The results of the structural investigations show that the mass of the spoiler structure is lower compared to a spoiler without SCB functionality. This fact is due to the area of the spoiler in which the support actuators are installed. In this area, no sandwich structure is required, but only a thin laminate. This laminate is even thinner than the upper and lower cover laminates of the reference sandwich structure combined, which is why this area is lighter. The stiffness in this area is provided by the support actuators. By using the support actuators a weight reduction of around 12% (3.4 kg) for the spoiler structure can be assumed. This reduces the influence of the additional mass from the support actuators by about 50%.

Regarding the system and structure analysis, it should be noted that certain elements are not considered within this analysis. Aspects like maintainability, repairability, and manufacturing are not taken into account. However, these aspects have a significant influence on the evaluation of new technologies and should therefore be included in further development steps.

For the evaluation on aircraft level, a simplified reference flight mission of a long-haul flight was defined within the project. This allows for the calculation of how much fuel can be saved due to the reduced drag of the improved aircraft. A detailed description of the work is given in [20]. The most important results are briefly summarized in this upcoming section.

By burning fuel the aircraft loses weight. To fly at the optimum lift coefficient, the aircraft would have to climb at a constant rate, since the reduced weight of the aircraft, due to the burned fuel, leads to a lower required density. However, this is not possible in modern flying with other traffic. Air traffic control defines altitude corridors within which the aircraft normally operates. To fly at an optimum lift coefficient with lower fuel consumption, the flight level can be changed in consultation with air traffic control. In the considered flight mission of this research, the flight levels FL340, FL360 and FL380 are used. The difference corresponds to approximately 610 m in each case. Assuming a take-off mass m_0 of 240,000 kg and the specific fuel consumption *SFC* of $1.4 * 10^{-5} \frac{kg}{Ns}$, the fuel consumed m_f can be calculated using the Breguet range equation

$$R = \frac{c_L}{c_D} * \frac{V}{g * SFC} * ln\left(\frac{m_0}{m_0 - m_f}\right). \quad (1)$$

The speed during the flight mission is indicated by *V* (Mach 0.85) and the ratio between lift and drag coefficient $\frac{c_L}{c_D}$ is 19.6. In comparison, $\frac{c_L}{c_D}$ for the aircraft without SCB functionality is 19.2. Based on the Breguet formula with the presented assumptions, a fuel saving of approximately 1,000 kg can be estimated for a long-haul flight (9,000 km).

4. CONCLUSION

In this work, the design of a new function in an existing wing was presented. For the implementation of the SCB functionality a concept was selected that minimally affects the overall aircraft system architecture. By using the existing systems, the complexity of the implementation was reduced. The concept was further developed by including the actuation concept for the application on an HLFC wing.

The conceptual design process of the SCB actuation system was outlined, demonstrating how system design can be undertaken at an early stage of introducing a new function. This interdisciplinary approach allows for the consideration of mass and performance impacts at an early design stage. Such an approach enables the formulation of preliminary assessments regarding the feasibility of integrating the new system into the overall aircraft.

A concept was developed that appears to be feasible from the aerodynamic, structural, and systems engineering perspectives. In terms of system technology, the critical factor identified was the available installation space for the support actuator. However, the additional mass introduced by the actuation system was deemed of secondary importance based on the analyses conducted. This is particularly because the incremental mass can be counterbalanced by the relatively low structural weight.

In forthcoming investigations, the feasibility of implementing the models needs to be ascertained in more detail. This requires a more in-depth refinement of the models followed by simulations and hardware testing. Moreover, it is essential to examine the system's impact on safety. Preliminary investigations in this regard have already been conducted in this project [21].

Besides the application of the method to the SCB system presented here, the basic procedure and the underlying models can also be employed for other designs. For instance, the procedure and individual models can also be applied to the design of other control surfaces actuation systems (e.g. ailerons). In this way, initial estimates of mass and installation space requirements can be made at an early design stage.

5. ACKNOWLEDGMENT

Funded by the Federal Republic of Germany. Funding source: Federal Ministry for Economic Affairs and Energy based on a resolution of the Bundestag. The project Move-IntegR (20W1729C) is part of the Federal Aeronautical Research Program (LuFo V-3).

REFERENCES

[1] D. S. Lee *et al.*, 'The contribution of global aviation to anthropogenic climate forcing for 2000 to 2018', *Atmospheric Environment*, vol. 244, p. 117834, 2021, doi: 10.1016/j.atmosenv.2020.117834.

[2] L. Dray *et al.*, 'Cost and emissions pathways towards net-zero climate impacts in aviation', *Nature Climate Change*, vol. 12, no. 10, pp. 956–962, 2022, doi: 10.1038/s41558-022-01485-4.

[3] N. Beck, T. Landa, A. Seitz, L. Boermans, Y. Liu, and R. Radespiel, 'Drag reduction by laminar flow control', *Energies*, vol. 11. 2018. doi: 10.3390/en11010252.

[4] M. Werner, 'Application of an adaptive shock control bump for drag reduction on a variable camber NLF wing', in *2018 AIAA aerospace sciences meeting*, 2018, p. 0789.

[5] J. Birkemeyer, H. Rosemann, and E. Stanewsky, 'Shock control on a swept wing', *Aerospace Science and Technology*, vol. 4, no. 3, pp. 147–156, 2000, doi: https://doi.org/10.1016/S1270-9638(00)00128-0.

[6] H. Ogawa, H. Babinsky, M. Pätzold, and T. Lutz, 'Shock-wave/boundary-layer interaction control using three-dimensional bumps for transonic wings', *AIAA journal*, vol. 46, no. 6, pp. 1442–1452, 2008.

[7] S. C. Künnecke, S. Vasista, J. Riemenschneider, R. Keimer, and M. Kintscher, 'Review of adaptive shock control systems', *Applied Sciences*, vol. 11, no. 2, p. 817, 2021.

[8] H. Hansen, J. Kirn, W. Machunze, C. Metzner and M. J. Weber, 'Aircraft wing with an adaptive shock control bump', US10,427,779B2, Oct. 01, 2019

[9] M. Kintscher, J. Riemenschneider, H.-P. Monner, and M. Wiedemann, 'Structural concept of an adaptive shock control bump spoiler', *CEAS Aeronautical Journal*, vol. 12, Apr. 2021, doi: 10.1007/s13272-021-00507-9.

[10] A. Goerttler, S. C. Künnecke, and C. Sabater, 'Aerodynamic design of shock control bumps considering structural constraints'23. *DGLR-Fachsymposium STAB*. Berlin, Nov. 2022.

[11] S. C. Künnecke, M. Schäfer, A. Goerttler, A. Waldmann, S. Vasista, and J. Riemenschneider,

‘Concept of a morphing shock control bump spoiler with two actuators’. *SMART 2023 - 10th ECCOMAS Thematic Conference on Smart Structures and Materials*, Patras, Greece, Jul. 2023.

[12] D. Scholz, ‘Development of a CAE-tool for the design of flight control and hydraulic systems’, Technical University Hamburg-Harburg, Germany, 1995.

[13] EASA, ‘CS-25 certification specifications and acceptable means of compliance for large aeroplanes’, *EASA*, 2016.

[14] D. van den Bossche, ‘The A380 flight control electrohydrostatic actuators, achievements and lessons learnt’, *ICAS-Secretariat - 25th Congress of the International Council of the Aeronautical Sciences 2006*, vol. 6. pp. 3383–3390, 2006.

[15] J.-C. Mare, *Aerospace actuators 2*. ISTE Ltd; John Wiley & Sons, 2017.

[16] D. Hagen, D. Padovani, and M. Choux, ‘Guidelines to select between self-contained electro-hydraulic and electro-mechanical cylinders’, May 2020. doi: 10.1109/ICIEA48937.2020.9248373.

[17] M. Budinger, J. Liscouët, F. Hospital, and J.-C. Maré, ‘Estimation models for the preliminary design of electromechanical actuators’, *Proceedings of the Institution of Mechanical Engineers, Part G: Journal of Aerospace Engineering*, vol. 226, no. 3, pp. 243–259, 2012, doi: 10.1177/0954410011408941.

[18] B. Yu, S. Wu, Z. Jiao, and Y. Shang, ‘Multi-objective optimization design of an electrohydrostatic actuator based on a particle swarm optimization algorithm and an analytic hierarchy process’, *Energies*, vol. 11, no. 9, 2018, doi: 10.3390/en11092426.

[19] T. Streit, M. Kruse, T. Kilian, J. V. Geyr, and I. Petropoulos, ‘AERODYNAMIC DESIGN AND ANALYSIS OF HLFC WINGS WITHIN THE EUROPEAN PROJECT HLFC-WIN’, *33rd Congress of the International Council of the Aeronautical Sciences, ICAS 2022*, vol. 1. pp. 127–150, 2022.

[20] A. Goerttler, ‘Aerodynamic design of shock control bumps on a transport aircraft wing considering structural constraints,’ *AIAA 2024-2133. AIAA SCITECH 2024 Forum,* Orlando. January 2024, doi: 10.2514/6.2024-2133.

[21] M. Schäfer, A. Berres, and O. Bertram, ‘Integrated model-based design and functional hazard assessment with SysML on the example of a shock control bump system’, *CEAS Aeronautical Journal*, vol. 14, no. 1, pp. 187–200, 2023, doi: 10.1007/s13272-022-00631-0.